Journal of the Technical University of Gabrovo

https://mc04.manuscriptcentral.com/jtug

COMPREHENSIVE MODEL OF THE MICRO-HARDNESS OF DIAMOND BURNISHED 41CR4 STEEL SPECIMENS

Vladimir Dunchev *

Technical University of Gabrovo, 5300 Gabrovo, Bulgaria

ARTICLE INFO

Article history:
Received 29 April 2020
Accepted 04 May 2020

Keywords:
diamond burnishing, micro-hardness, experimental design, mathematical model

ABSTRACT

Diamond burnishing (DB), based on severe plastic deformation of the surface layer, improves the surface integrity (SI) of metal components and thus, enhances their operating properties. The micro-hardness is one of the mechanical characteristics of the SI. The increased micro-hardness due to DB is a precondition for improved wear and fatigue crack resistance of the treated component. The article presents a comprehensive experimental mathematical model which predicts the micro-hardness distribution in depth from the surface depending on the diamond insert radius and burnishing force. The selection of the significant governing factors is based on previous study. The experimental model is based on a fourth-order one-dimensional polynomial whose variable is the depth and the coefficients are functions of the two governing factors.

1. INTRODUCTION

The aim of the mechanical surface treatment processes based on surface plastic deformation is significant improvement of the operating properties of the treated metal component – fatigue strength, wear resistance, corrosion resistance and so on. One of the static processes is slide burnishing (SB) at which the contact between the deforming element and surface being treated is sliding friction. When the deforming element is made of diamond (artificial or natural), the method is referred to as diamond burnishing (DB). Due to the severe surface plastic deformation caused by DB, the surface integrity (SI) of the diamond burnished component is improved significantly which reflects positively on the operating properties of the corresponding component. One of the mechanical characteristics of the SI is the micro-hardness. The increased micro-hardness due to DB intervention is a precondition for improved wear and crack resistance of the treated component.

In the last two decades, a number of studies have focused on the effect of SB, and in particular DB, on the micro-hardness of both nonferrous metals and alloys, and steels. Bednarski et al. [1] investigated the effect of DB on the micro-hardness distribution in A1Mg1SiCu aluminum matrix composite. The used synthetic diamond was composed of diamond grains and a ceramic bonding phase, namely titanium silicon carbide Ti3SiC2. Using Taguchi L18 orthogonal array, Buldum and Cagan [2] studied the surface micro-hardness of slide burnished AZ91D magnesium alloy. The effect of the burnishing force, feed rate, burnishing velocity and number of passes was established. Czechowski and Tobola [3] obtained the micro-hardness distribution in aluminum matrix composites subjected to DB. Multi-response optimization of SB of 7075 AA for an optimal parametric combination to yield favorable surface roughness and microhardness was conducted by Esme [4] using the Grey relational analysis and Taguchi's method. The governing factors were the burnishing force, feed rate, burnishing velocity and number of passes. Gharbi et al. [5] studied the effect of the burnishing force and feed rate on the surface micro-hardness of 1050A aluminum, subjected to SB. Regression models of the surface micro-hardness of LY12 AA and H62 brass, subjected to DB, were established by Luo et al. [6]. The depth of penetration, feed rate and burnishing velocity were chosen as governing factors. The effect of the additional parameters (number of passes, working scheme and lubricant used) of DB process on the micro-hardness distribution in 2024-T3 AA was studied by Maximov et al. [7]. Tanaka et al. [8] reported that the surface micro-hardness of 7075 AA was improved with more than 100HV due to DB intervention. Teimouri et al. [9] studied the surface hardness of 6061-T6 AA subjected to ultrasonic assisted SB. On the basis of an experimental design these authors established regression model of the surface hardness. The effect of the governing factors on the hardness was investigated. Boguslaev et al. [10] investigated the effect of DB (using I-20A oil as lubricant) on the surface micro-hardness of Kh12NMBF-Sh steel with coating. Using the one-factor-at-the-time technique these authors established the influence of the burnishing force and feed rate on the surface micro-hardness. Two types of tool steels with adhesive coatings and diffusion layers, namely Vanadis 6 and Vanadis 10, were subjected to DB and the surface microhardness was studied by Brostow et al. [11]. The effect of the diamond radius and burnishing

* Corresponding author. E-mail: v.dunchev@tugab.bg

velocity on the surface microhardness was established by these authors. Hamadache et al. [12] studied the effect of the burnishing force, feed rate, burnishing velocity and number of passes on the surface micro-hardness, using the one-factor-at-the-time technique, of diamond and roller burnished Rb40 (wich corresponds to AISI 1335) steel specimens. These authors established that, as a whole, DB ensures higher surface micro-hardness. Hamadache at al. [13] reported that the initial micro-hardness HRA of 36CrNiMo6 steel can be increased from 66.35 to 71.33. Ultrasonic SB with wolfram-carbide ball of 3mm in diameter was investigated by Huuki and Laakso [14], who tested the surface micro-hardness of 34CrNiMo6-M tempered steel. DB with a cylindrical-ended deforming element of 42Cr4Mo steel was studied by Korzynski et al. [15]. On the basis of an experimental design and regression analysis, these authors obtained a model of the surface micro-hardness with the following variables: diameter of the deforming element, burnishing force and feed rate. Lobanowski and Ossowska [16] obtained the micro-hardness distribution in UR52N duplex stainless steel, subjected to DB, for three magnitudes of the burnishing force. Maximov et al. [17] investigated the spherical motion burnishing of 37Cr4 specimens. These authors established the micro-hardness distribution for three values of the hoop linear strain. The one-factor-at-the-time technique was applied by Maximov et al. [18] on diamond burnished AISI 316Ti chromium-nickel steel specimens in order to study the surface micro-hardness. The burnishing velocity, number of passes and working scheme were chosen as governing factors. These authors reported that with increasing the velocity, the surface micro-hardness decreases. At velocity of $v = 200\,m/min$ the measured micro-hardness (387 HV 0.05) was less than that of the base specimen, processed only by cutting (412 HV0.05). At burnishing velocity of $v = 50\,m/min$ the surface micro-hardness increased with 14.6%. Radziejewska and Skrzypek [19] developed a new hybrid method - SB (sintered carbides as deforming elements) combined with laser alloying process. These authors reported that the new method significantly increased the surface micro-hardness of 45carbon steel, coated with cobalt satellite layer (300μm in depth). Sachin et al. [20-22] investigated the effect of DB process parameters on the micro-hardness of 17-4PH stainless steel under cryogenic, minimum quantity lubrication and dry environments. Saldana-Robles et al. [23] reported that SB of AISI 1045 steel increased the surface micro-hardness with 14%. Shiou et al. [24] investigated the SB (a tungsten carbide rod with a ground polished sphere-shaped end as a deforming element) of SUS420J2 (equivalent to AISI420) stainless steel. These authors reported for increasing the surface hardness (HRC) with several units. Tanaka et al. [25] reported that the surface micro-hardness of SUS316 stainless steel was improved with more than 300HV due to DB intervention. Tobola et al. [26, 27] investigated the effect of DB (diamond composites with ceramic bonding phase, namely Ti3SiC2) and subsequent nitriding on the micro-hardness distribution in depth of treated AISI D2 tool steel and tempered tool steels - Sverker 21 and Vnadis 6. These authors showed that the combination of nitriding and DB significantly increased the micro-hardness.

Based on the conducted literary survey, the following conclusion can be drawn: Missing a comprehensive mathematical model, which can reliably predict the micro-hardness distribution in depth from the surface layer, due to DB of medium carbon low alloy steel, carried out with a different combination of the values of the governing factors. The main purpose is to obtain and investigate such a model. The paper is devoted only on modeling the influence of the significant basic parameters of the DB process on micro-hardness distribution in depth form the surface layer.

2. MATERIAL AND METHOD OF STUDY

2.1. Specimen material

The experiments were conducted on specimens made of 41Cr4 steel. This steel is a typical representative of the medium- carbon, low-alloy steels and used widely in engineering practice. The steel was received as $\phi 22\,mm$ bar stocks with lengths of $3000\,mm$. The batch chemical composition, which we established is listed in Table 1. Tensile tests were carried out on cylindrical specimens with a gauge diameter of $6\,mm$. The fatigue limit was established via rotating bending fatigue tests. The average mechanical characteristics, shown in Table 2, were established in our “Testing of Metals” laboratory.

Table 1 *Chemical composition of the tested 41Cr4 steel*

Element	C	Si	Mn	Cr	P	S	Cu	Ni	Al	Ti	Mo	Fe
wt%	0.41	0.25	0.71	0.93	0.012	0.012	0.28	0.09	0.024	0.022	0.015	Balance

Table 2 *Mechanical characteristics of 41Cr4 steel*

Young modulus E, MPa	Yield limit $R_{0.2}, MPa$	Ultimate stress R_m, MPa	Elongation $A_5, \%$	Transverse contraction $z_t, \%$	Fatigue limit σ_{-1}, MPa
200000	*789*	*986*	*10.3*	*26*	*440*

2.2. Specimen preparation

The specimens were manufactured on a CNC T200 lathe using a special burnishing device mounted on the tool post of the lathe (Fig. 1). A polycrystalline diamond tool with spherical tip was supported elastically within the device. The required burnishing force was set by deforming an axial spring situated in the device with linear behaviour. The deforming diamond was brought into contact with the specimen at its centerline and normal to the surface being treated. The device was then fed into the specimen an additional $0.05\,mm$ to allow the diamond tool to become disengaged from the stop in the device. The latter was then fed along the surface of the rotating specimen to produce a burnished surface using the lubricant Hacut 795-H.

Four workpieces were used to produce the micro-hardness specimens. Each workpiece was designed for DB of four cylindrical surfaces with different burnishing forces,

but with a constant radius of diamond insert according to Fig. 1. The initial workpieces had a length of $160\ mm$ and diameter of $20\ mm$. Each workpiece was clamped to one side with the chuck and supported on the other side. Turning and DB were conducted in one clamping process to minimize the concentric run-out in burnishing. The turning was conducted from end to end for each workpiece using a DNMG 50608 – RF carbide cutting insert. The length treated via DB using one and the same combination of governing factors was $20\ mm$. DB was implemented with a constant feed rate of $f = 0.05 mm/rev$ and burnishing velocity of $v = 100 m/min$, but with different combinations of diamond radii and burnishing forces. Finally, four micro-hardness specimens were cut from each workpiece or total of 16 specimens.

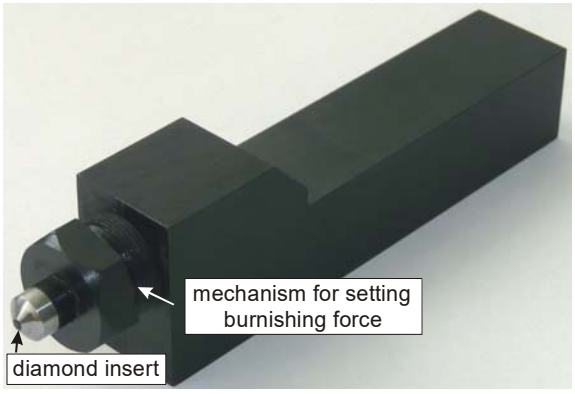

Fig. 1. DB device

2.3. Micro-hardness measurements

The micro hardness was measured via $ZHV\mu$ microtester. After DB the specimens were cross sectioned and the micro-hardness distribution in depth from the surface was measured. The additional measurements on the cylindrical surface of the specimens were conducted in order to complete the micro-hardness distribution.

For each cylindrical specimen (experimental point from the experimental design) the surface micro-hardness was measured along to six equidistant to one another generatrixes belonging to the cylindrical surface. Ten measurements were taken for each generatrix or a total of 60 measurements per specimen. For each specimen a statistical graph of the measurements is made and the scattering interval and the center of clustering (median) are found. The result corresponding to the median is accepted as the final result for the surface micro-hardness of the corresponding specimen

For each specimen, the depth of the hardened layer is determined by the following algorithm:

1) One of the two face surfaces of each specimen is polished;

2) The micro-hardness is measured along to eight equally spaced radial directions, in depth of 1 mm from the surface with increments of 0.05 mm;

3) For each depth from the surface multiple of 0.05 mm, the arithmetic mean of the results of the eight measurements is calculated; for each specimen the measured surface micro-hardness is added to the resulting database;

4) The resulting database for the micro-hardness distribution for each specimen is visualized in „microhardness – depth of hardened layer" coordinate system;

5) For each specimen the arithmetic mean of the micro-hardness is calculated in a depth from the surface in 0.3-1 mm interval. This arithmetic mean is adopted to be initial micro-hardness;

6) For each specimen the hardened layer depth is defined by the intersection of the initial micro-hardness and the HV=HV(depth) graphics.

3. PROPOSED MODEL

3.1. Experimental design

A planned experiment was conducted. On the basis of previous study, the radius r and burnishing force F_b were chosen to be governing factors. Their levels are listed in Table 3. The feed rate and the burnishing velocity were chosen as $f = 0.05 mm/rev$ and $v \le 100 m/min$. The experimental design is shown in Table 4.

3.2. Experimental results

The distribution in depth from the surface layer of the measured micro-hardness (in red) as well as the result from the initial micro-hardness for each experimental point is shown in Fig. 2.

Table 3 *Governing factors and their levels*

Governing factors		Levels of the factors Coded			
		-1	-0.333	+0.333	+1
Naturals $\tilde{x}_i$	Coded x_i	Natural			
Diamond radius $r\ [mm]$, $\tilde{x}_1$	x_1	2	3	4	5
Burnishing force $F_b\ [N]$, $\tilde{x}_2$	x_2	100	200	300	400

Table 4 *Experimental design*

Exp. point	1	2	3	4	5	6	7	8
x_1	-1	-1	-1	-1	-0.333	-0.333	-0.333	-0.333
x_2	-1	-0.333	0.333	1	-1	-0.333	0.333	1
Exp. point	9	10	11	12	13	14	15	16
x_1	0.333	0.333	0.333	0.333	1	1	1	1
x_2	-1	-0.333	0.333	1	-1	-0.333	0.333	1

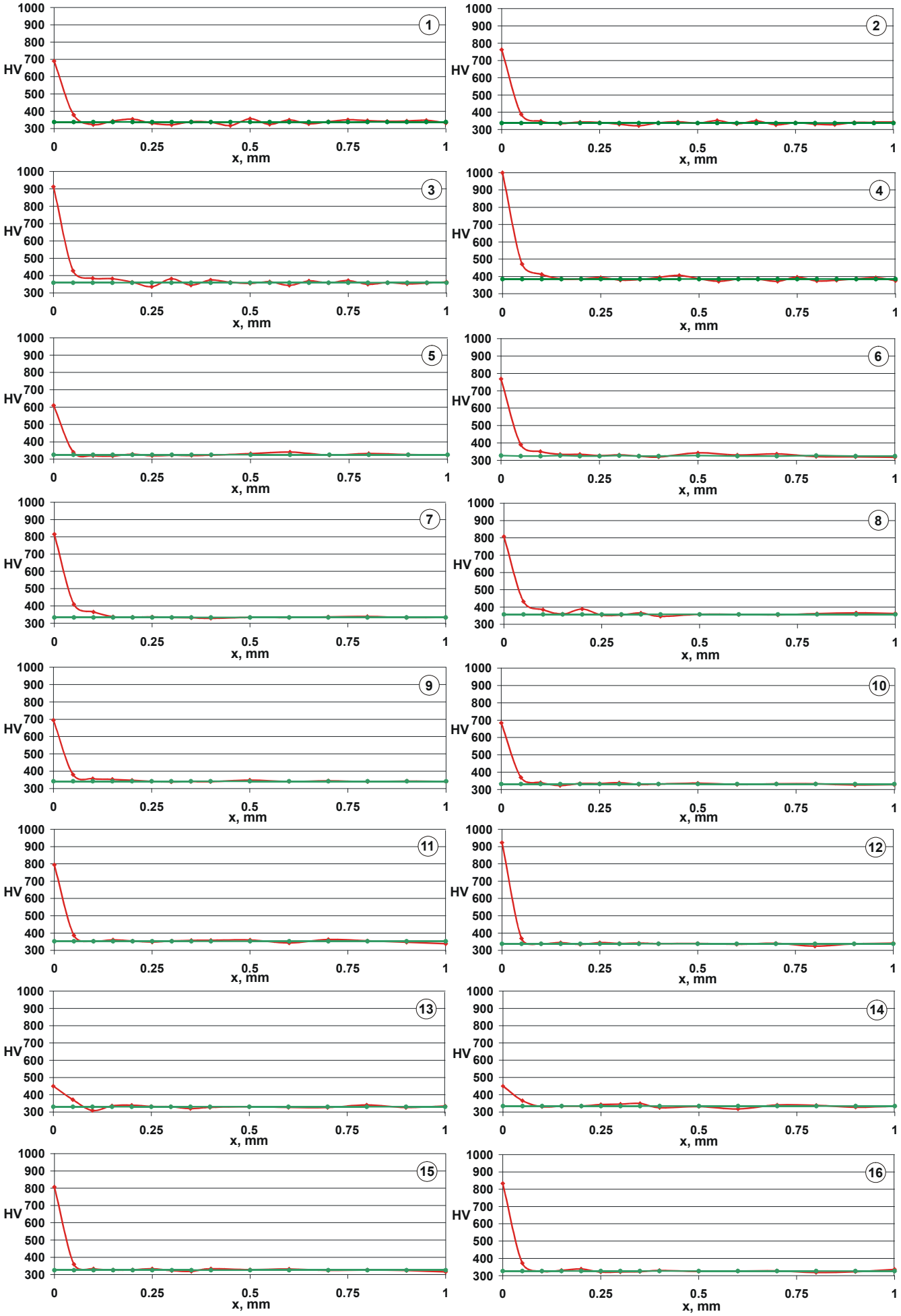

Fig. 2. Micro-hardness distribution experimental results and the initial micro-hardness

Table 5 *Magnitudes of the coefficients* $a_{i,j}$

Exp. point	1	2	3	4	5	6	7	8
$a_{0,j}$	690	762	912	1000	610	768	815	808
$a_{1,j}$	-12505	-7239.5	-18438	-25832	-10523	-13792	-13709	-12638
$a_{2,j}$	167527	-127805	229967	462081	119223	158769	129865	118210
$a_{3,j}$	-881136	3000000	-1000000	-4000000	-240530	-728251	-337615	-307385
$a_{4,j}$	893939	-20000000	2000000	10000000	-2000000	1000000	-401282	-348718
Exp. point	9	10	11	12	13	14	15	16
$a_{0,j}$	694	684	795	923	450	450	807	834
$a_{1,j}$	-12173	-11774	-19592	-12161	-1704.9	-3222.2	-18071	-21437
$a_{2,j}$	155800	142482	341646	-168185	-13467	39819	222598	356405
$a_{3,j}$	-838667	-712410	-3000000	5000000	452433	-184028	-707253	-3000000
$a_{4,j}$	2000000	1000000	7000000	-30000000	-3000000	-69444	-2000000	6000000

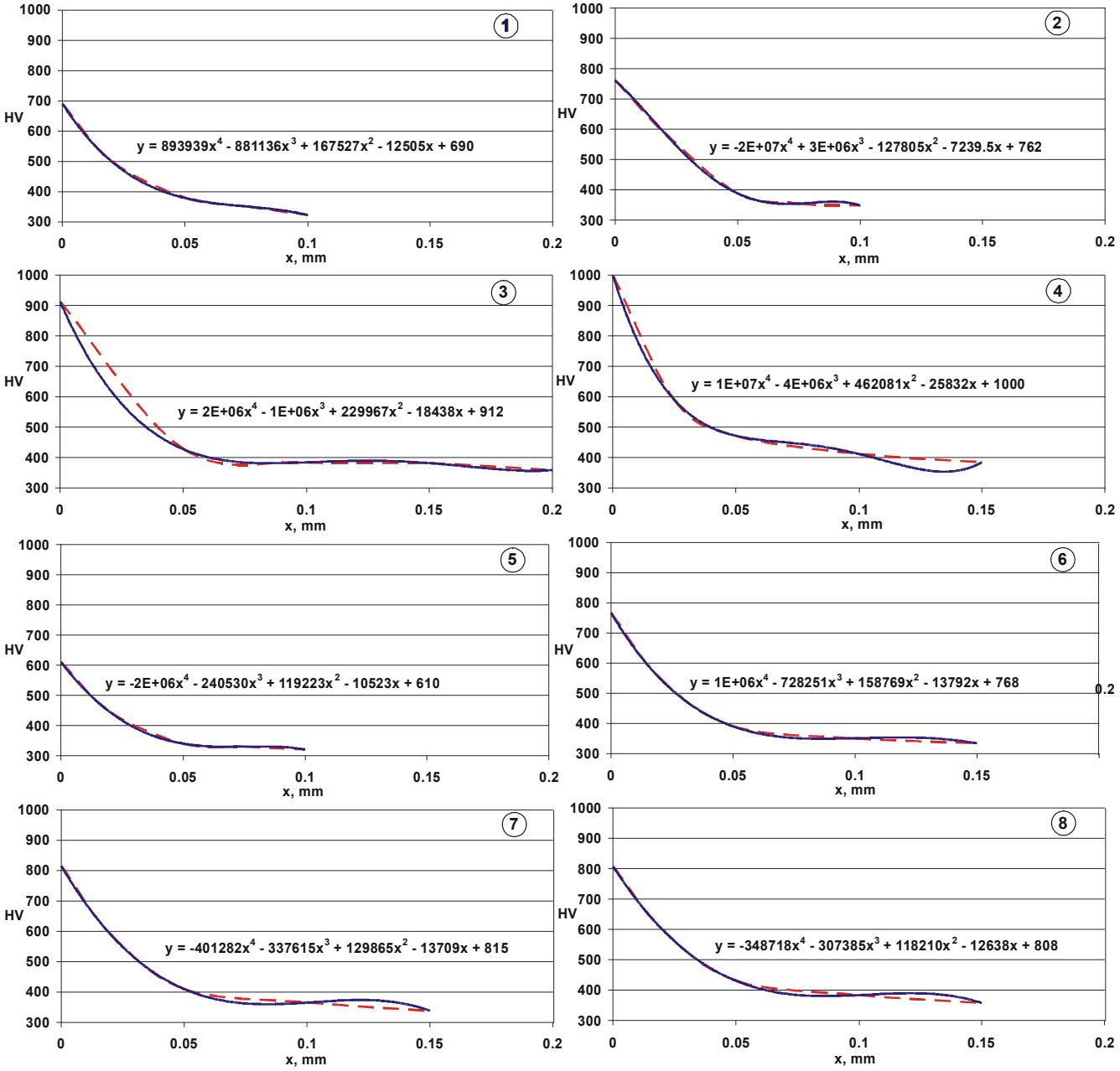

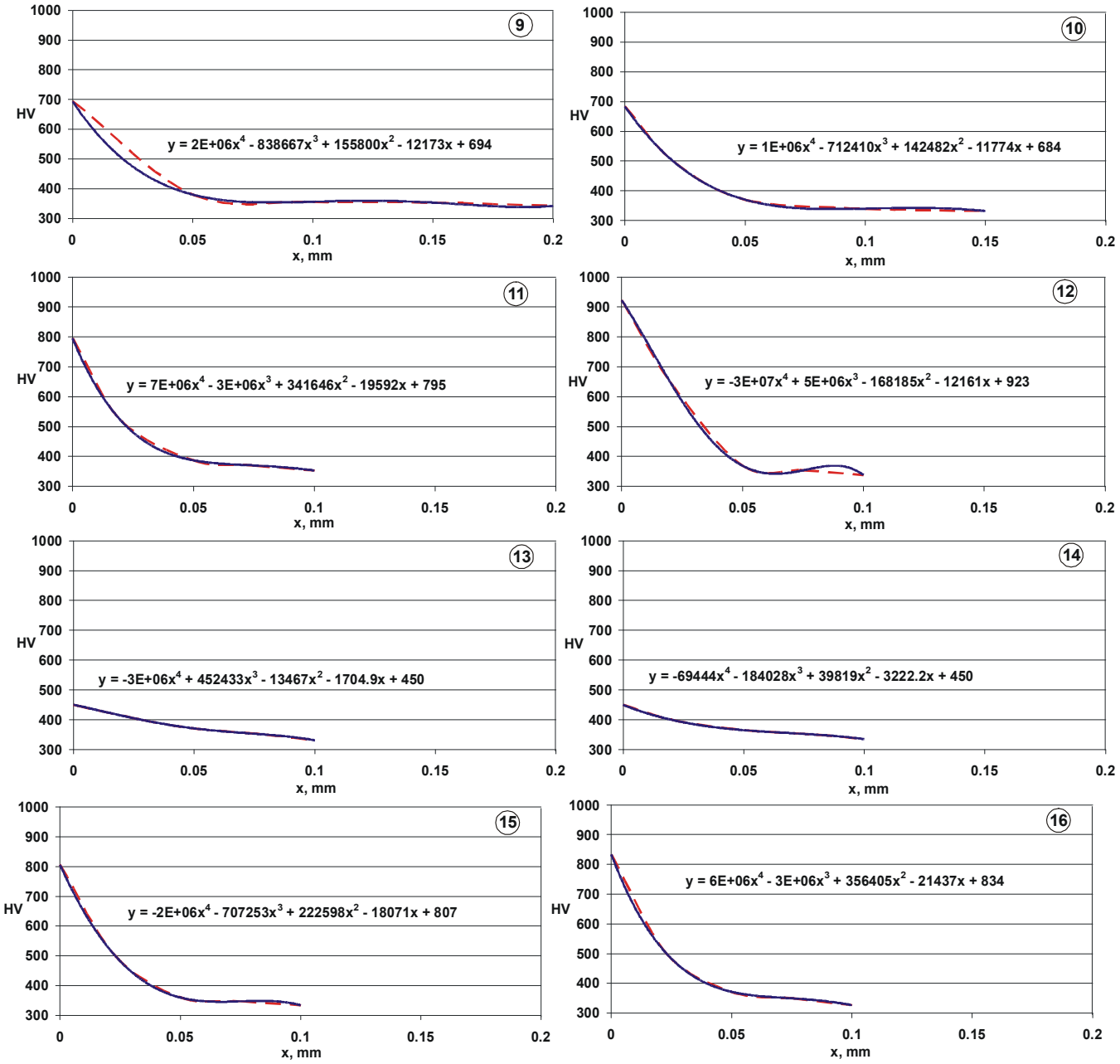

Fig. 3. Comparison between the experimental micro-hardness distribution in depth and the approximations

3.3. Synthesis of the model

Each experimental distribution (for each experimental point from the experimental design) was approximated via a polynomial of n-th order in relation to the depth d:

$$HV_j = a_{0,j} + \sum_{i=1}^{n} a_{i,j} d^i , \quad (1)$$

where the coefficient $a_{i',j}$, $i' = 0,1,2,...,n$, in fact, depend on the chosen governing factors:

$$a_{i',j} = a_{i',j}(x_1, x_2), \; j = 1,2,...,16 . \quad (2)$$

Polynomial of fourth-order was chosen. The coefficients $a_{i,j}$ are shown in Table 5. Figure 3 shows a comparison between the experimental data and the approximations (see eq. (1)). In the approximations the variable "x" corresponds to the depth "d", while the function "y" corresponds to the microhardness "HV_j". The experimental results are depicted with interrupted red lines.

Therefore, the desired comprehensive model of the micro-hardness distribution can be written as:

$$HV = a_0(x_1, x_2) + \sum_{i=1}^{n} a_i(x_1, x_2) d^i \quad (3)$$

In order to determine the functions $a_{i'} = a_{i'}(x_1, x_2)$, where $i' = 0,1,2,...,n$, $n+1$ in number regression analyses were conducted, based on Table 4, using QStatLab software. Since the governing factors were had four levels (see Table 4), the regression models were chosen to be polynomials of degree no larger than three. In order to perform the correct statistical analyses, the number of coefficients in the polynomials should not exceed the number of experimental points, i.e., 16. The following models were obtained for the $a_{i'} = a_{i'}(x_1, x_2)$ functions:

$$a_{i'} = b_{0,i'} + \sum_{k=1}^{q} b_{k,i'} x_k + \sum_{k=1}^{q-1} \sum_{\ell=k+1}^{q} b_{k\ell,i'} x_k x_l + \sum_{k=1}^{q} b_{kk,i'} x_k^2 + \sum_{k=1}^{q-1} \sum_{\ell=k+1}^{q} b_{kk\ell,i'} x_k^2 x_l + \sum_{k=1}^{q} b_{kkk,i'} x_k^3 \qquad (4)$$

where $q = 2$ is the number of the variables. The coefficient $b_{0,i'}, ..., b_{kkk,i'}$ are shown in Table 6.

Thus, Eq. (3) and (4), and Table 6, define the micro-hardness distribution. Figure 4 shows the comparison between the experiment and the micro-hardness, predicted by the proposed model. It should be noted that physical meaning have only these magnitudes of HV, which are larger than initial micro-hardness (before diamond burnishing). An additional limitation is the depth of distribution to be equal or smaller to 0.2 mm. As a whole, the proposed model shows a good agreement compared to the experimental data, especially near to the surface layer.

The comprehensive model obtained allows to be established the micro-hardness distribution for a combination of the governing factors, which are optimal under given criterion (for instance, minimum roughness, maximum fatigue limit, maximum wear resistance and so on).

Table 6 *Polynomial coefficient values* $b_{kkk,i'}$

	$b_{0,i'}$	$b_{1,i'}$	$b_{2,i'}$	$b_{11,i'}$	$b_{22,i'}$	$b_{12,i'}$	$b_{111,i'}$	$b_{222,i'}$	$b_{112,i'}$	$b_{122,i'}$
a_0	765.118	52.939	209.405	-26.993	0	32.484	-155.814	-123.156	96.997	0
a_1	-13425.72	-4078.161	-8505.007	0	0	-1577.801	48.79.668	9319.175	-9378.85	2963.246
a_2	114731.22	62716.69	138368.25	47704.252	8470.961	-13211.14	5162.479	-252378.4	281645.95	-150656
a_3	-53859.62	-199381.5	-839814.4	-724758.5	-20487.88	505186.35	-949265.4	2598147.4	-3345552	1942467.5
a_4	-2572350	-2933405	3069022	2189616.2	-700707.4	-3739664	8834967.3	-12135889	13568476	-8816156

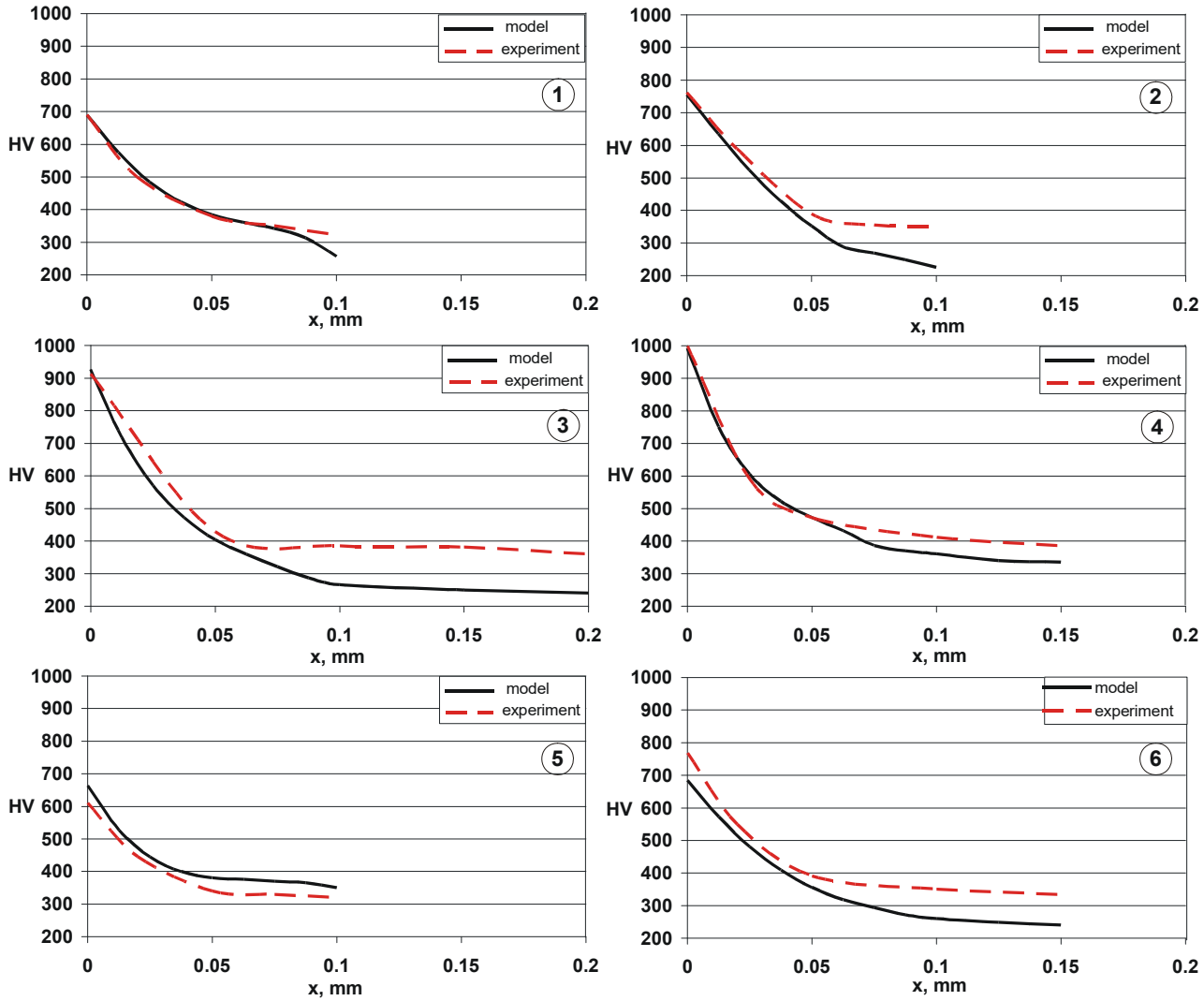

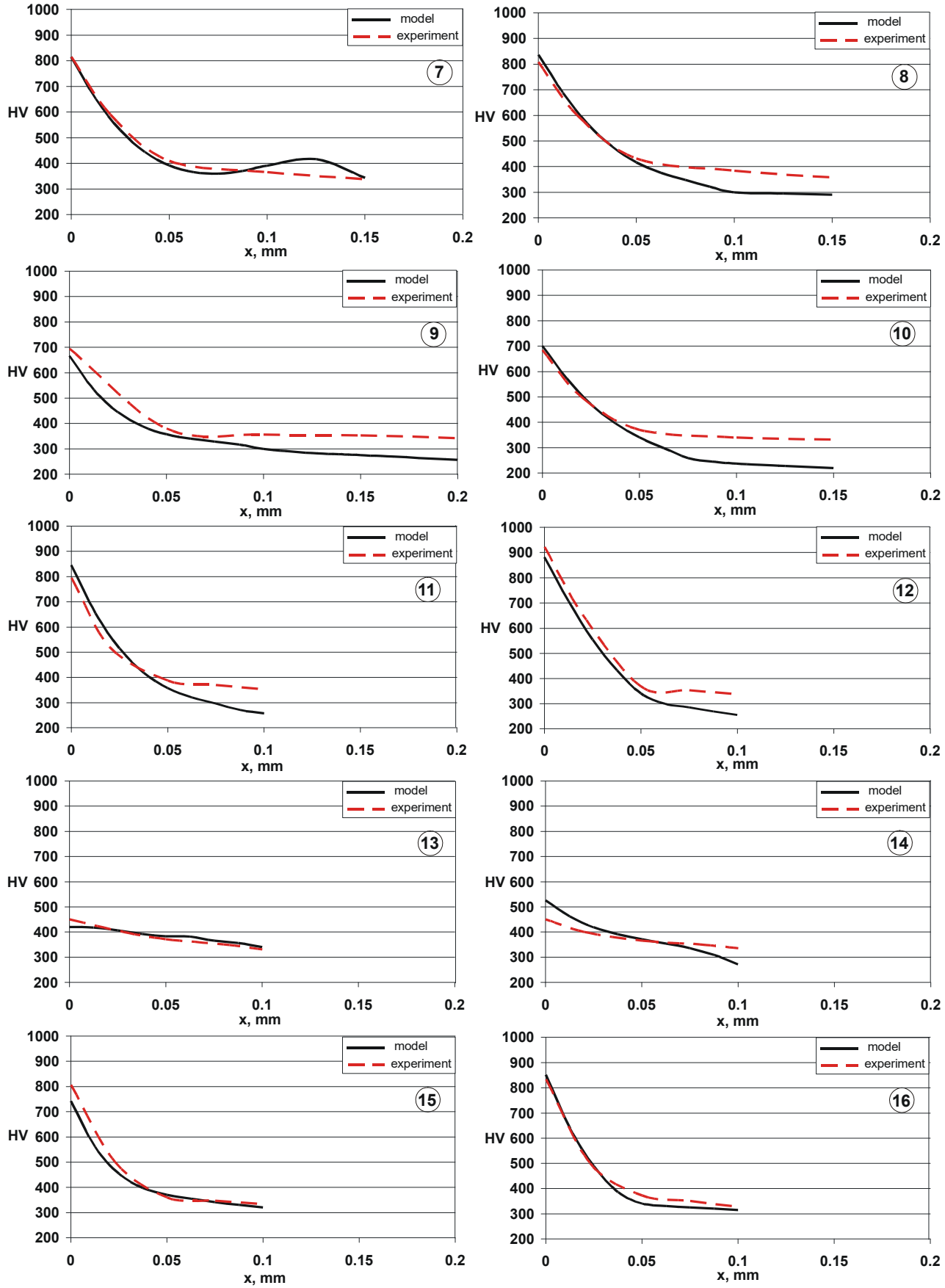

Fig. 4. Comparison between the experiment and the micro-hardness, predicted by the proposed model

4. CONCLUSIONS

The following conclusions can be made:

• A comprehensive experimental mathematical model, which predicts the micro-hardness distribution in depth from the surface in 41Cr4 steel diamond burnished components, has been developed. The governing factors are the diamond insert radius and burnishing force.

• The comprehensive model obtained allows to be established the micro-hardness distribution for a combination of the governing factors, which are optimal

under given criterion (for instance, minimum roughness, maximum fatigue limit, maximum wear resistance and so on).

ACKNOWLEDGMENT

This work was supported by the European Regional Development Fund within the OP „Science and Education for Smart Growth 2014-2020", Project CoC "Smart Mechatronics, Eco- and Energy Saving Systems and technologies", №BG05M2OP001-1.002-0023.

REFERENCES

[1] Bednarski P., Bialo D., Brostow W., Czechowski K., Polowski W., Rusek P., Tobola D. Improvement of tribological properties of matrix composites by means of slide burnishing. Materials Science 19(4) (2013) 367-372

[2] Buldum B.B., Cagan S.C. Study of Ball Burnishing Process on the Surface Roughness and Microhardness of AZ91D Alloy. Experimental Techniques 42(2) (2018) 233-241

[3] Czechowski K., Tobola D. Slide finishing burnishing of metal alloys and metal matrix composites. Mechanik NR (7) (2017) 1-3

[4] Esme U. Use of grey based Taguchi method in ball burnishing process for the optimization of surface burnishing and microhardness of AA7075 aluminium alloy. Materials and Technology 44 (2010) 129-135

[5] Gharbi F., Sghaier S., Hamdi H., Benameur T. Ductility improvement of aluminum 1050A rolled sheet by a newly designed ball burnishing tool device. International Journal of Advanced Manufacturing Technology 60(1-4) (2012) 87-99

[6] Luo H., Liu J., Wang L., Zhong Q. The effect of burnishing parameters on burnishing force and surface microhardness. The International Journal of Advanced Manufacturing Technology 28(7-8) (2006) 707-713

[7] Maximov J.T., Anchev A.P., Duncheva G.V., Ganev N., Selimov K.F. Influence of the process parameters on the surface roughness, micro-hardness, and residual stresses in slide burnishing of high-strength aluminum alloys. Journal of the Brazilian Society of Mechanical Sciences and Engineering 39(8) (2017) 3067-3078

[8] Tanaka H., Ishii W., Yanagi K. Optimal Burnishing Conditions and Mechanical Properties of Surface Layer by Surface Modification Effect Induced of Applying Burnishing Process to Stainless Steel and Aluminum Alloy. Journal of the Japan Society for Technology of Plasticity 52(605) (2011) 726-730 (in Japanese)

[9] Teimouri R., Amini S., Bami A.B. Evaluation of optimized surface properties and residual stress in ultrasonic assisted ball burnishing of AA6061-T6. Measurement 116 (2018) 129-139

[10] Boguslaev V.A., Yatsenko V.K., Yakovlev V.G., Stepanova L.P., Pukhalskaya G.V. The effect of diamond burnishing on structure and properties of detonation-gas coatings on gas-turbine engine parts. Material Science and Heat Treatment 50(1-2) (2008) 44-48

[11] Brostow W., Czechowski K., Polowski W., Rusek P., Tobola D., Wronska I. Slide diamond burnishing of tool steels with adhesive coatings and diffusion layers. Materials Research Innovation 17(4) (2013) 269-277

[12] Hamadache H., Laouar L., Zeghib N.E., Chaoui K. Characteristics of Rb40 steel superficial layer under ball and roller burnishing. Journal of Materials Processing and Technology 180(1-3) (2006) 130-136

[13] Hamadache H., Zemouri Z., Laouar L., Dominiak S. Improvement of surface conditions of 36CrNiMo6 steel by ball burnishing process. Journal of Mechanical Science and Technology 28(4) (2014) 1491-1498

[14] Huuki J., Laakso S.V.A. Integrity of surface finished with ultrasonic burnishing. Proc IMechE Part B: J Engineering Manufacture 227(1) (2013) 45-53

[15] Korzynski M., Lubas J., Swirad S., Dudek K. Surface layer characteristics due to slide diamond burnishing with a cylindrical-ended tool. Journal of Materials Processing Technology 211 (2011) 84-94

[16] Lobanowski J., Ossowska A. Influence of burnishing on stress corrosion cracking susceptibility of duplex steel. Journal of Achievemens in Material and Manufacturing Engineering 19(1) (2006) 46-52

[17] Maximov J.T., Kuzmanov T.V., Duncheva G.V., Ganev N. Spherical motion burnishing implemented on lathes. International Journal of Machine Tools and Manufacture 49 (2009) 824-831

[18] Maximov J.T., Duncheva G.V., Anchev A.P., Ganev N., Amudjev I.M., Dunchev V.P. Effect of slide burnishing method on the surface integrity of AISI 316Ti chromium-nickel steel. J Braz. Soc. Mech. Sci. Eng. (2018) 40: 194. https://doi.org/10.1007/s40430-018-1135-3

[19] Radziejewska J., Skrzypek S. Microstructure and residual stresses in surface layer of simultaneously laser alloyed and burnished steel. Journal of Materials Processing Technology 209 (2009) 2047–2056

[20] Sachin B., Narendranath S., Chakradhar D. Effect of cryogenic diamond burnishing on residual stress and microhardness of 17 – 4 PH stainless steel. Materials Today 5(9) Part 3 (2018) 18393-18399

[21] Sachin B., Narendranath S., Chakradhar D. Experimental evaluation of diamond burnishing for sustainable manufacturing. Materials Research Express 5(10) (2018) 106514 (DOI: 10.1088/2053-1591/aadb0a)

[22] Sachin B., Narendranath S., Chakradhar D. Sustainable diamond burnishing of 17-4 PH stainless steel for enhanced surface integrity and product performance by using a novel modified tool. Mater. Res. Express 6 (2019) 046501

[23] Saldana-Robles A., Plascencia-Mora H., Aguilera-Gomez E., Saldana-Robles A., Marquez-Herrera A., Diosdado-De la Pena J.A. Influnce of ball-burnishing on roughness, hardness and corrosion resistance of AISI 1045 steel. Surface & Coatings Technology 339 (2018) 191-198

[24] Shiou F.J., Huang S.J., Shin A.J., Zhu J., Yoshino M. Fine Surface Finish of a Hardened Stainless Steel Using a New Burnishing Tool. Procedia Manufacturing 10 (2017) 208-217

[25] Tanaka H., Ishii W., Yanagi K. Optimal Burnishing Conditions and Mechanical Properties of Surface Layer by Surface Modification Effect Induced of Applying Burnishing Process to Stainless Steel and Aluminum Alloy. Journal of the Japan Society for Technology of Plasticity 52(605) (2011) 726-730 (in Japanese)

[26] Tobola D., Brostow W., Czechowski K., Rusek P., Wronska I. Structure and properties of burnished and nitrided AISI D2 tool steel. Materials Science 21(4) (2015) 511-516

[27] Tobola D., Brostow W., Czechowski K., Rusek P. Improvement of wear resistance of some cold working tool steels. Wear 382-383 (2017) 29-39